NANOINDENTATION TESTING OF HUMAN ENAMEL AND DENTIN

#RADOSLAV HALGAŠ*, **, JÁN DUSZA**, JANA KAIFEROVÁ***,
LUCIA KOVÁCSOVÁ***, NEDA MARKOVSKÁ***

*Faculty of Material Science and Technology of STU, Paulínska 16, 917 24 Trnava, Slovakia
**Institute of Materials Research of SAS, Watsonova 47, 040 01 Košice, Slovakia,
***1st Department of Stomatology of UPJS, Trieda SNP 1, 041 66 Košice, Slovakia

#E-mail: radoslav.halgas@stuba.sk

Submitted March 4, 2013; accepted June 17, 2013

Keywords: Human enamel, Dentin, Nanoindentation, AFM, Microstructure

The objective of this investigation is to characterize the indentation behaviour of human enamel and dentin using instrumented indentation methods. The experiment was realized in different conditions; at indentation loads from 5 mN to 400 mN, loading rates from 10 to 1000 mN/min and constant loads from 10 to 400 mN for 1000 s. The indentation hardness (H_{IT}), reduced modulus (E_{IT}), and influence of applied load and loading rate on hardness and the creep behaviour have been evaluated. The hardness of enamel is the highest at its occlusal surface, decreases towards the dentin-enamel junction (DEJ) and has the lowest value at DEJ. The maximum value of H_{IT} was 6.53 ± 1.12 GPa in enamel and 1.08 ± 0.11 GPa in dentin. The average reduced modulus EIT was 92.86 ± 3.86 GPa and 22.95 ± 0.08 GPa in enamel and dentin, respectively. A significant load--size effect has been found during testing the hardness of enamel. The indentation load rate had only a minor influence on the penetration depth/energy loss of enamel. The creep deformation of enamel at 10 and 400 mN and 1000 s is 70 nm and 160 nm, respectively, with stress exponent n = 1.8.

INTRODUCTION

The human tooth consists of two calcified tissues, namely, enamel and dentine. Enamel, on the outer surface can be considered as a natural optimised coating, is the hardest tissue in the human body, comprising ~95 vol. % of apatite crystals and ~5 vol. % of water and organic materials arranged in ~5 µm keyhole-shaped structures known as prisms [1-3]. Prisms are aligned and run approximately perpendicular from the dentin-enamel junction to the tooth surface [4-6]. Each prism is separated from each other by a nanometer-thin layer of a protein-based organic matrix [7, 8]. Enamel protects the underlying dentine, retains its shape, as well as resisting fracture and wear damage during load-bearing function for the life of the individual, and acts as the cutting and grinding surface during mastication.

Dentin is composed of 70 wt. % inorganic material, 18 wt. % organic matrix and 12 wt. % water [9]. It is distributed throughout the crown and root, and so forms the bulk of the tooth and has the function of absorbing and distributing stresses within the tooth. Dentin has a distinct microstructure characterized by the presence of tubules (~1.5 µm in diameter) that run from the dentin-enamel junction towards the pulp [7, 10]. The tubules are surrounded by highly mineralized cylinders of peritubular dentin, roughly 0.5-1 µm in thickness, composed largely of apatite. These tubules are separated by intertubular dentin that consists of a hydrated matrix of type I collagen which is reinforced with a nanocrystalline carbonated apatite [9]. The structural and compositional dissimilarities between the enamel and dentin induce significant differences in their mechanical behaviour [11].

The sharp interface between materials with different elastical and mechanical properties is usually subjected to concentrated stresses which often cause delamination. In the case of human teeth a tight and durable junction known as the dentine–enamel junction (DEJ) exists between the two calcified tissues which persist throughout millions of cycles of mastication forces during the working life of a tooth, with only rare cases of mechanical damage. The DEJ has been described as a complex interface with at least three levels of microstructure: the 25-100 µm scallops with their convexities directed towards the dentine and concavities towards the enamel; the 2-5 µm micro-scallops housed within each scallop; and a finer nano-level structure within each micro-scallop, [8, 11]

Knowledge of the mechanical and tribological properties of human teeth is of importance as they act as a mechanical device during masticatory processes such as the cutting, tearing and grinding of food [4, 12, 13]. Teeth are exposed to a range of different loadings: firstly, they are in direct contact with other objects and/or opposing teeth and they encounter normal and sliding contact which results in wear. The masticatory forces range from tens of newtons to a thousand newtons and the contact area can be as small as a few square millimetres. The knowledge of properties such as hardness, elastic modulus, fatigue, etc, allows one to develop biomimetic restorative materials or improved oral treatments, and to comprehend the effect of the wide variety of restorative or aesthetic dental procedures [14]. An accurate understanding of the structure–properties relationship governing the DEJ would have significant clinical relevance and may permit the creation of improved interfaces between restorations and the odontogenic mineralized tissues.

During recent years, depth-sensing indentation has become a popular technique for mechanical characterization of mineralized biological tissues, including human enamel and dentin [15-24].

He and Swain [20] in their review papers summarized the possible mechanisms responsible for the excellent mechanical properties of enamel, including its hierarchical structure and the nanomechanical properties of the minor protein macromolecular component. According to their results, enamel shows a lower elastic modulus, higher energy absorption ability and greater indentation creep behaviour in comparison to the sintered hydroxyapatite. Cuy et al. [7] used nanoindentation for mapping mechanical properties of human molar teeth enamel. They found the enamel surface hardness, $H_{IT} > 6$ GPa and reduced modulus, $E_{IT} > 115$ GPa, while at the enamel–dentine junction $H_{IT} < 3$ GPa and $E_{IT} < 70$ GPa. Chuenarrom et al. [21] studied the effect of variations in indentation load and time on the Knoop and Vickers hardness of enamel and dentin. According to the results, a difference in indentation time did not influence the microhardness of enamel and dentin, but this was affected by variation of test loads. Braly et al [22] designed and performed an experiment to compare hardness and Young's modulus data for distinct prism orientations in enamel, both perpendicular to the long axes of the prisms and parallel to the axes of prisms by testing two mutually perpendicular surfaces near a common edge. They found that there is effectively no difference between the hardness and Young's modulus values for different prism orientations.

Brauer et al. [23] studied the effect of asymmetry in nano- and micromechanical properties of dentine. They reported a gradual increase in mechanical properties with increasing distance from the DEJ. Results suggest that dentine nano- and micromechanical properties vary with the tooth side in agreement with recent literature using macroscopic methods. On the other hand, Angker at all. [24] reported the opposite behaviour as regarding the hardness and elastic modulus of dentin in dependence on the location of indentation.

The aim of this investigation is to characterize hardness, elastic modulus, the load size effect of hardness, load rate effect on deformation and indentation creep of human teeth using instrumented indentation.

EXPERIMENTAL

Materials and methods

Four extracted non-carious human permanent molars from females aged 19-23 years required extractions as part of dental treatment were used in the present experiment. The patients were informed and consented to the use their teeth. Prior to processing, the teeth were stored in salt solution at 4°C to prevent demineralization. The growth of microorganisms in the medium was prevented by disinfection in 3 % hydrogen peroxide for 1 minute. The teeth were sectioned, using a precise diamond - bladed saw (STRUERS), into two halves of lingual and buccal (Figure 1) which were then embedded into cold EpoFix20 epoxy cold-mounting compound (Buehler Ltd., Lake Bluff, IL). Cutting parameters were: low speed rotation (150 rt./min) and cooling with water to protect dehydration and heating.

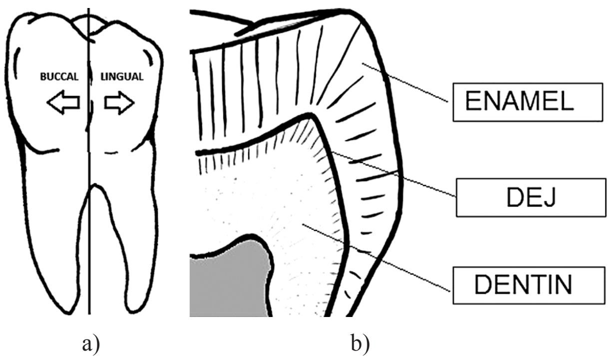

Figure 1. Schematic drawing of molar cut (a) with it's characteristic parts (b).

The mounted specimens were polished sequentially with 6-, 3-, 1- μm diamond paste and 0.25 μm alumina suspension to achieve a surface roughness of ~150 nm, as measured by mechanical profilometry. Between polishing steps, the samples were gently cleaned to remove any debris. During the entire preparation process, the samples were kept in salt solution except during grinding and polishing so as to maintain hydration of the samples. With the aim of visualization of the microstructure of enamel and dentin, specimens were etched with citric acid (10 %) solution. Light microscopy (LM), scanning electron microscopy (SEM) and atomic force microscopy (AFM) were used for the characterization of human enamel and dentin microstructure.

The indentation tests were performed using an instrumental hardness tester (TTX/NHT by CSM Instruments) equipped with a Berkovich indenter. Indentation hardness, H_{IT}, reduced modulus, E_{IT}, influence of the applied loads and loading rates on hardness and creep deformation at room temperature have been studied. For H_{IT} and E_{IT} measurements across the tooth in enamel, DEJ area and dentin, a single load indentation was used at 25 mN and 300 mN at a loading rate of 50 mN/min.

The indentation hardness and reduced modulus were automatically calculated using the Oliver-Pharr method [19]. The first indents were located near the occlusal surface of enamel, followed by indents toward DEJ and then in dentin. At the least, 3 measurements were realized at every distance from the occlusal surface of enamel. To investigate the load size effect during the hardness measurement, experiments were performed under different loads. The central area of enamel and dentin was impressed with loads of 5/10/20/50/100/200 and 400 mN. The minimum spacing of indents was 25 mm. The average values of hardness and reduced elastic modulus were calculated from at least three independent measurements. To study the influence of loading rates on hardness, three different loading rates of 10, 100 and 1000 mN/min have been used. The indents were located in the centre of enamel vertically to the enamel prisms at a maximum applied load of 100 mN.

A Berkovich indenter was used to investigate the indentation creep behaviour of enamel at an applied load of 10, 50, 100 and 400 mN and hold time of 1000 seconds. Each test condition with the same load and time was performed three times. Measurements were situated in the centre of the enamel, vertically to the prisms and the minimum spacing of indents was 25 mm.

RESULTS AND DISCUSSION

In human enamel studied the basic microstructure block was observed in the form of so-called ‘key hole shaped’ enamel rods with diameter approximately 5 mm, Figure 2a, c. The shape and size of these rods are different at the different locations of the enamel from the occlusal surface towards the DEJ but always are arranged parallel in a direction perpendicular to the DEJ. The smallest structural units are in the form of a needle or plate like hydroxyapatite crystallites which are roughly rectangular in cross section with a mean width of approximately 100 nm and mean thickness of approximately 50 nm. At this level, the directional arrangement of the hydroxy-apatite crystallites varies, and plates in the central part of the rod are parallel to the rod axis while those near the edge of the rod usually have an angle of 30-50 degrees to the longitudinal axis of the rods, Figure 2b. The main structural features of dentin are the dentin tubules with diameters from 1.5 to 3 mm, which extend through the entire dentin thickness, but vary both in number and diameter along the thickness of the dentin, Figure 2e, f.

In Figure 3 the load-penetration depth curves of the indents applied in three different regions of enamel are illustrated. Examination of the results reveals that, under the same load, the penetration depth was the deepest (~2.45 μm) in the region near the DEJ. In the inter region of enamel, at approximately half distance between DEJ and occlusal surface of enamel, the penetration depth was ~2.25 μm. The penetration depth exhibits the lowest value in the region close to the occlusal surface of enamel with a value of 2.2 μm. These results indicate that the region near the DEJ is more deformable than the outer enamel region. Very similar results were presented by He and Swain [2] after testing premolar teeth at a 25 mN load.

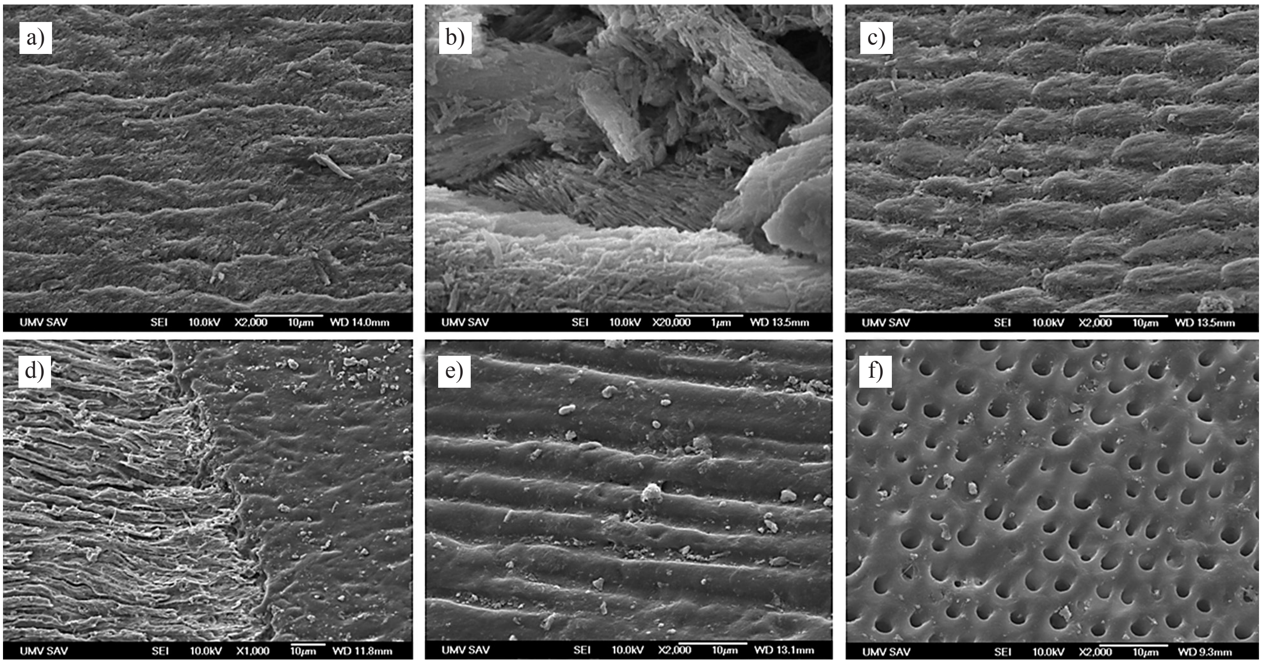

Figure 2. Characteristic structure of the human tooth investigated on it’s cross section. Occlusal area of enamel with typical prismatic structure of enamel rods (a), detail of HAP particles in enamel prism (b), central area of enamel (c), DEJ between enamel on the left side (rough) and dentin on the right (smooth) (d), parallel section of dentine and tubules (e) and vertical section of dentin (f).

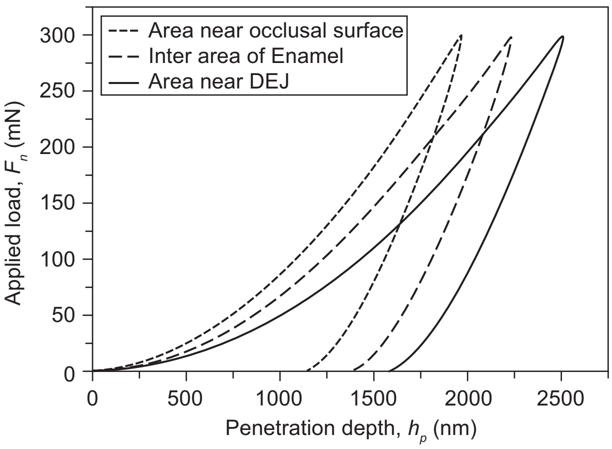

Figure 3. Comparison of $F - h_p$ curves in different areas of enamel.

The results from indentation experiments that traverse the entire length of the cross-sectioned enamel-DEJ-dentin sample are illustrated in Figure 4a-b. The hardness of enamel is significantly higher (Figure 4a) in comparison to that of dentin with values different for the area close to the surface ~6.5 GPa and area close to the DEJ ~3.5 GPa. The hardness of dentin is significantly lower in comparison to the enamel with an average value of ~1 GPa. Similar behaviour was found in the case of reduced modulus in Fig. 4b with a decrease in its value from the enamel surface ~90 GPa to DEJ ~75 GPa. There is a significant change in reduced modulus crossing the DEJ from ~75 GPa to ~20 GPa. Cuy et al. [7] used nanoindentation for mapping mechanical properties of human molar teeth enamel. They found the hardness of enamel at it's surface, $H_{IT} > 6$ GPa and reduced modulus, $E_{IT} > 115$ GPa, while at the enamel–dentine junction, $H_{IT} < 3$ GPa and $E_{IT} < 70$ GPa. He and Swain [20] also used nanoindentation for characterisation of the hardness of enamel. Their results are similar as the results of Cuy et al., but with slightly lower values of hardness and reduced modulus.

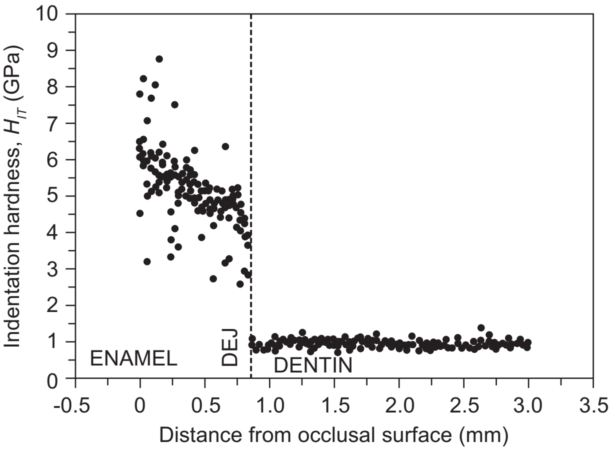

a)

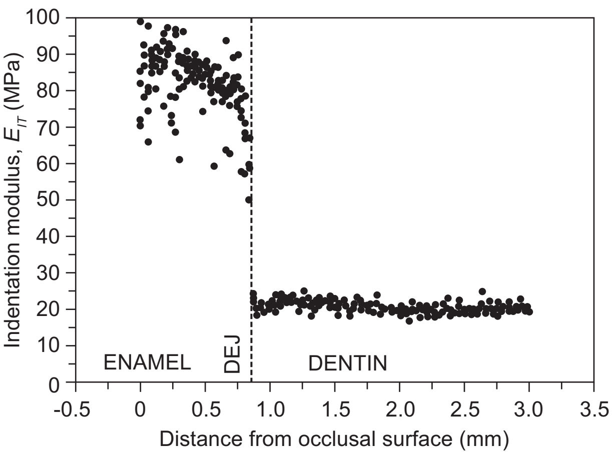

b)

Figure 4. Indentation hardness - H_{IT} (a) and reduced modulus - E_{IT} (b) of cross – section from outer surface to dentin, crossing EDJ.

Chan et al. [4] during an experiment similar to the present work found enamel to have an elastic modulus of ~95 ± 15 GPa and a hardness of 7 ± 2 GPa, whereas dentine had an elastic modulus of ~19 ± 2 GPa and hardness of 1 ± 0.1 GPa. A sharp change in mechanical properties was observed across the DEJ, similarly as it was found during the present investigation. Braly et al. [22] designed and performed an experiment to compare hardness and Young's modulus data for distinct prism orientations in enamel. The geometrically small sample used allowed for the measurement of Young's modulus and hardness of a chemically similar group of prisms in separate orientations parallel and perpendicular to the long axes of the prisms. The indentation experiments show no significant difference in the mechanical properties measured perpendicular or parallel to the prisms in enamel however these results do not preclude a difference in these properties when tested by other methods. It seems that the variations in hardness mapped by previous researchers using indentation studies are predominantly due to variations in chemistry across the enamel and not due to variations in prism orientation.

In Figure 5 AFM images of the indents are illustrated, created with same indentation load in enamel, at DEJ and in dentin. The indents exhibit different size as evidence of the different hardness of these regions.

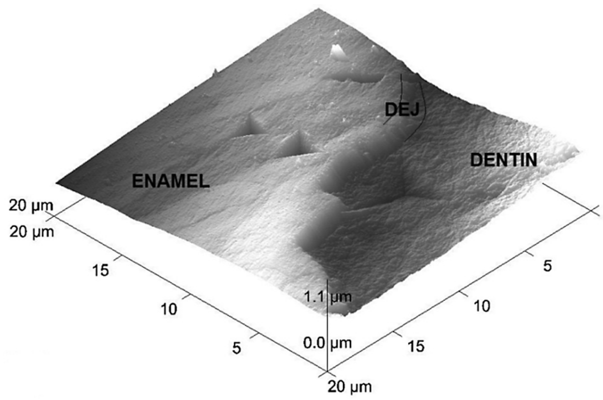

Figure 5. Indents created with the same load at the DEJ in the enamel and dentin side.

Results of Brauer et al. [23] revealed a gradual increase in mechanical properties with increasing distance from the DEJ. Coronal dentine showed higher elastic modulus and hardness on the lingual side of teeth for all measurements, while root dentine was harder on the buccal side. This increase in the case of dry teeth was observed up to a distance of 200 microns from the DEJ. On the other hand, Angker at all. [24] reported opposite behaviour. The mean hardness and elastic modulus of the dentine nearest the pulp wall was 0.52 ± 0.24 and 11.59 ± 3.95 GPa, respectively, which was significantly lower than those of dentine in the middle area, which was 0.85 ± 0.19 and 17.06 ± 3.09 GPa, respectively, and the dentine nearest DEJ, which was 0.91 ± 0.15 and 16.33 ± 3.83 GPa, respectively. Our results show no significant change in the hardness of dentin during the indentation of areas with different distances from the DEJ.

The influence of applied indentation load on hardness values, measured in the inter region of enamel and dentin, are illustrated in Figure 6, respectively. The hardness of enamel decreases from ~6.0 GPa to ~3.5 GPa with an increased indentation load from 5 mN to 400 mN. A similar tendency was observed in dentin, where the hardness decreased from ~1.1 GPa to ~0.7 GPa with an increasing load from 5 mN to 400 mN. With the aim to find the true-hardness values for enamel and dentin, the relationship h_c versus F_n was constructed in Figure 7. The modified PSR model [25] provides for the calculation of the true- hardness and the values of 3.5 GPa and 0.6 GPa have been obtained for the true-hardness enamel and dentin, respectively.

Luis et al. [14] studied the elastic modulus and hardness variability of enamel and dentin for bovine teeth by nanoindentation using single indentation (SI) and continuous stiffness measurement (CSM). Similar indentation loads have been used as in our experiment from 1 mN to 500 mN. Both elastic modulus and hardness decreased with increased indentation load. Hardness values for enamel from ~5 GPa to ~1.5 GPa and for dentin from ~1.1 GPa to ~0.6 GPa have been reported by SI method. The CSM method resulted in slightly lower hardness values at low indentation loads and higher at higher indentation loads. The hardness values of human tooth enamel reported in the present work are very similar to the hardness of bovine enamel at low indentation loads ~5 mN, however there are higher values at high indentation loads around 400 mN. In regards to hardness of human dentin, our investigation is in good agreement with the hardness of bovine dentin reported by Luis et al. [14].

To explain this so called "indentation load/size effect ISE" intensive research has been performed during the last decade and several theories have been occurred for explanation of this effect, [26, 27]. The most common explanation concerns the experimental errors resulting from the limitations of the resolution of the objective lens and the sensitivity of the load cells. Other explanation is that the ISE is directly related to the intrinsic structural factors of the materials investigated, including indentation elastic recovery, work hardening during indentation, surface dislocation pinning, etc. It was found that dislocation and twin activities may results in ISE in alumina ceramics with different grain size, too. Another explanation of ISE is the formation of cracks, small ratios of grain size to the indentation size.

Park et al. [28] realized and investigation with the aim to quantify and compare the brittleness and load size effect of human enamel and common dental restorative materials used for crown replacement. The hardness, elastic modulus and apparent fracture toughness were characterized as a function of distance from the DEJ using indentation approaches. These properties were then used in estimating the brittleness according to a model that accounts for the competing dissipative processes of deformation and fracture. The brittleness of selected porcelain, ceramic and micaceous glass ceramic dental materials was estimated and compared with that of the enamel. The average brittleness of the young (approximately 20 years) and old (approximately 50 years) enamel increased with distance from the DEJ.

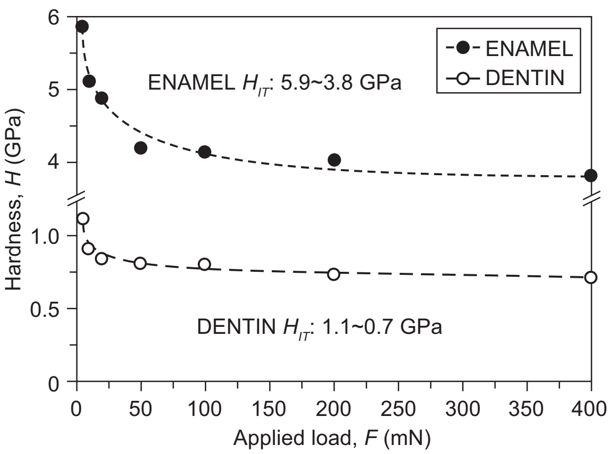

Figure 6. Load size effect of hardness in enamel and dentine at different loads from 5 to 400 mN.

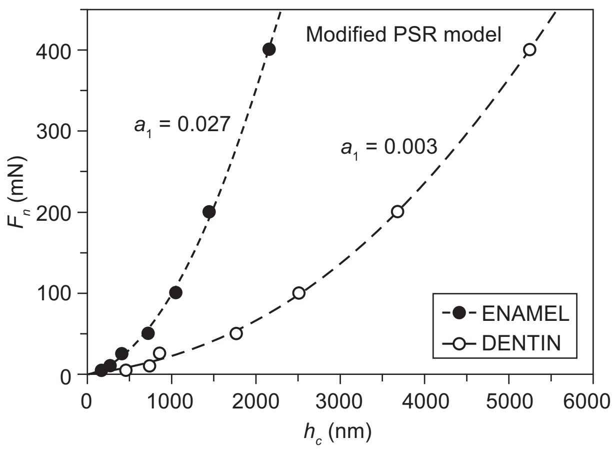

Figure 7. Indentation size versus the peak load for enamel and dentin.

For the old enamel the average brittleness at occlusal surface was three times higher as at the DEJ. While there was no significant difference between the two age groups at the DEJ, the brittleness of the old enamel was up to four times higher than that of the young enamel near the occlusal surface. The brittleness numbers for the restorative materials were up to 90 % lower than that of young occlusal enamel. They found approximately 1.0 mN for the value of indentation load, above which the indentation hardness of enamel is load independent.

The structure-property relationship in human adult and baby teeth was characterised by grazing-incidence synchrotron radiation diffraction, optical and atomic-force microscopy and Vickers indentation by Low et al. [29]. Human adult and baby teeth exhibited distinct similarities that included; progressive decrease in hardness from enamel to dentine, load-dependent hardness for enamel but load-independent for dentine, time independent hardness for both enamel and dentine and cracks formation in enamel at higher loads but not in dentine. To understand the crack propagation in human teeth is an important field of research, too. The crack propagation in bovine enamel, dentin and DEJ was investigated by Bechtle et al [30, 31] using bending bars and correlated crack profile analysis. The phenomenon of crack propagation was explained via the elastic modulus mismatch between enamel and dentin that was found to highly influence stress intensities around crack tips in the DEJ bimaterial bending bars. This study suggests that the DEJ itself is a very well-bonded and strong interface since cracking along the DEJ occurred rather seldom. They found that the preferred crack propagation path in enamel is the protein rich interface between enamel rods and inter rod region. It was reported that the enamel exhibits rising fracture resistance behaviour with value from 0.8 - 1.5 MPam$^{1/2}$ at the beginning of crack propagation up to 4.4 MPam$^{1/2}$ at 500 mm crack extension. No significant difference was observed between the fracture resistance behaviour of enamel depending on sample orientation.

The force-displacement loading curves applied in the centre of enamel at 100 mN maximal load and different loading rates are illustrated in Figure 8. At the 100 mN load the lowest indentation rate results in the highest penetration depth of ~0.1 μm and the highest rate in the lowest depth of 0.08 μm. The results indicate that there is only a slight difference between the penetration depths at a different loading rate despite a 100-fold difference in the loading rates. This indicated that the energy loss ratio for enamel is almost strain rate independent. Similar results were presented by He and Swain [32], who found that the force rate had only a minor influence on the energy loss of enamel and the energy loss with a Berkovich indenter was greater than with a spherical indenter at an equivalent contact strain. This low dependence of energy loss as a consequence of loading rate suggests that enamel viscous behaviour is not the major basis of the energy loss mechanism. Enamel has a prism microstructure composed primarily of aligned hydroxyapatite crystallites with a very thin protein layer between them surrounded by a thicker organic rich sheath. Taking to the consideration the nano-sized building blocks of the enamel with very high theoretical strength and the probably maximal stresses in the vicinity of the indenter we can exclude from the consideration that energy loss by conventional dislocation based plastic deformation of the inorganic phase is important for enamel. Based on the results of investigations on nacre and bone three different mechanisms were considered by He and Swain [32] to contribute to the measured energy absorption; fluid flow within the sheath structure, protein ‟sacrificial bond" extension and nanoscale friction within sheaths associated with the degustation of enamel rods. Further work is required to understand and describe the energy loss mechanisms in human enamel, [33 -36].

The creep behaviour of enamel is described in Figure 9, where the influence of indentation load and

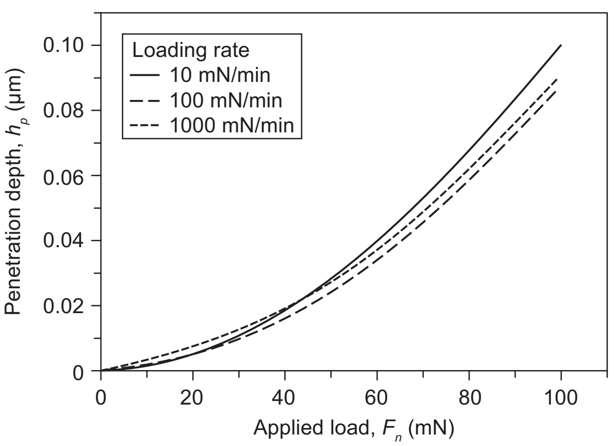

Figure 8. Comparison of $F - h_p$ curves at different force loading rates.

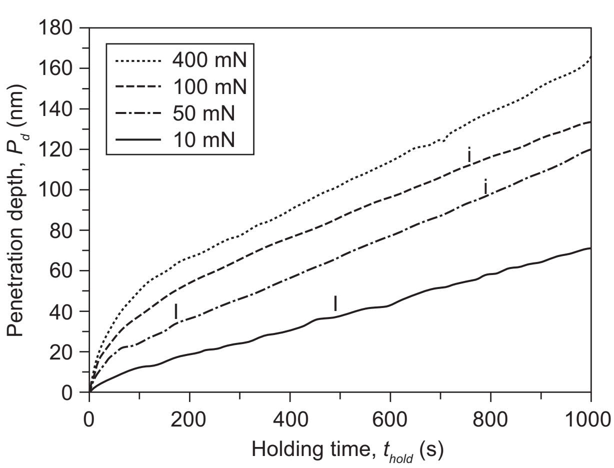

Figure 9. Creep curves of enamel at different applied loads.

holding time on the penetration depth is illustrated. The illustrated penetration depth is a relative value which was calculated by subtracting the initial depth at the beginning of the holding time. The primary creep region is increasing with the increasing indentation load and changing from approximately 25 to 200 seconds. The penetration depth at 1000 sec. holding time is approximately 70 nm at the indentation load of 10 mN, 120 nm at 50 mN, 130 nm at 100 mN and 160 nm at the indentation load of 400 mN.

The strain rate is plotted against stress, and the resulting curve analyzed to deduce a value for stress exponent n = 1.8, as shown in Figure 10. These results are in good agreement with the results of He and Swain [37] who measured the creep deformation of inner and other region of enamel and reached approximately 80 nm penetration depth at 900 sec. at 100 mN indentation load. This is slightly lower in comparison to our result (~120 nm). They found a significantly wider primary creep region and less sharp boundary between the primary and secondary creep regions in comparison to our results.

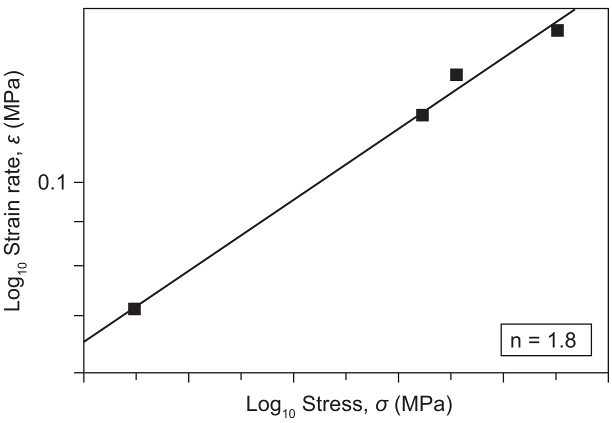

Figure 10. Stress exponent of strain rate - ε against stress - σ.

The creep behaviour of metals and ceramics together with the creep behaviour of polymers has been well described over the last decades, [38-40]. There are, however, only limited investigations dealing with the creep/ indentation creep behaviour of human enamel and dentin, [37, 41-44]

Enamel has different creep mechanisms than what occurs in metals or ceramics because of its totally different chemical composition, mainly related to the organic protein components existing between the apatite crystallites. He and Swain [37] compared the mechanical responses of enamel with dental-used materials and found that enamel exhibited a much more extensive creep response than HAp. They concluded that creep behaviour of enamel comes mainly from the protein films between the apatite crystallites and the prisms and the limited creep response of enamel can be explained by the fact, that protein films occupy only a very small volume fraction of the entire enamel. Future investigations will explain in more detail the creep behaviour of enamel and dentin and the applicability of the indentation creep technique in this area of research.

CONCLUSION

The aim of this investigation is to characterize the indentation behaviour of human teeth using instrumented indentation. The main conclusions are the following:

- The hardness of enamel is the highest at its occlusal surface, decreases towards the DEJ and has the lowest value at DEJ.
- The maximum value of H_{IT} was 6.53 ± 1.12 GPa in enamel and 1.08 ± 0.11 GPa in dentin. The maximum reduced modulus E_{IT} was 92.86 ± 3.86 GPa and 22.95 ± 1.08 GPa in enamel and dentin, respectively.
- Significant load-size effect has been found during the testing of enamel hardness, the hardness decreased from ~6.0 GPa to ~3.5 GPa when the indentation load increased from 5 mN to 400 mN.
- The indentation load rate had only a minor influence on the penetration depth/energy loss of enamel.
- The creep behaviour of enamel at applied loads of 10, 50, 100 and 400 mN exhibits a relatively short primary creep region and a pronounced secondary region with a stress exponent of n = 1.8.

Acknowledgment

Work was supported by the project Slovak Grant Agency for Science, grant No. 2/0122/12 by the Nano-CEXmat I. ITMS no:262200120019, NanoCEXmat II., ITMS no: 26220120035, CeKSiM, ITMS no:26220120056 APVV-0520 -10, APVV-0042 06 and CE SAS CLTP-MREC.

REFERENCES

1. Lu C., Nakamura T., Kroach Ch.S.: J. Biomech. *45*, 1437 (2012) .
2. He L.H., Swain M.V.: J. Dent. *37*, 596 (2009).
3. He B., Huang S., Zhang C., Jing J., Hao Y., Xiao L., Zhou X.: Arch. Oral Biol. *56*, 997 (2011).
4. Chan Y.L., Ngan A.H.W., King N.M.: J. Mech. Behav. Biomed. *4*, 785 (2011).
5. Marshall Jr. G.W., Balooch M., Gallagher R.R., Gansky S.A., Marshall S.J.: J. Biomed. Mater. Res. *54*, 87 (2001).
6. Ten Cate A.R.: *Oral Histology: Development, Structure and Function*, Mosby, St. Louis, MO, 1994.
7. Cuy J.L., Mann A.B., Livi K.J., Teaford M.F., Weihs T.P.: Arch. Oral. Biol. 47, 281 (2002).
8. Habelitz S., Marshall S.J., Marshall Jr. G.W., Balooch M.: Arch. Oral. Biol. *46*, 173 (2001).
9. Giannini M., Soares C.J., Marins de Carvalho R.: Dent. Mater. *20*, 322 (2004).

10. Marshall Jr G.W., Marshall S.J., Kinney J.H., Balooch M.: J. Dent. *25*, 441 (1997).
11. Marshall S.J., Balooch M., Habelitz S., Balooch G., Gallagher R., Marshall G.W.: J. Eur. Ceram. Soc. *23*, 2897 (2003).
12. Roy S., Basu B.: Mater. Charact. *59*, 747 (2008).
13. Kishen A., Ramamurty U., Asundi A.: J. Mech. Behav. Biomed. *51*, 650 (2000).
14. Giráldez de Luis I., Garrido M.A., Gómez-del Río T., Ceballos L., Rodríguez J.: Bol. Soc. Esp. Ceram. *49*, 177 (2010).
15. Oyen M.L.: J. Biomech. *39*, 2699 (2006).
16. Balooch G., Marshall G.W., Marshall S.J., Warren O.L., Asif S.A.S., Balooch M.: J. Biomech. *37*, 1223 (2004).
17. Ang S.F., Scholz T., Klocke A., Schneider G.A.: Dent. Mater. *25*, 1403 (2009).
18. He L.H., Swain M.V.: Dent. Mater. *23*, 814 (2007).
19. Oliver W.C., Pharr G.M.: J. Mater. Res. *7*, 1564 (1992).
20. He L.H., Swain M.V.: J. Mech. Behav. Biomed. *1*, 18 (2008).
21. Chuenarrom Ch., Benjakul P., Daosodsai P.: Mater. Res-Ibero-AM. J. *12*, 473 (2009).
22. Braly A., Darnell L.A., Mann A.B., Teaford M.F., Weihs T.P.: Arch. Oral Biol. *52*, 856 (2007).
23. Brauer D. S., Hilton J.F., Marshall G.W., Marshall S.J.: J. Biomech. *44*, 1626 (2011).
24. Angkera L., Swain M.V., Kilpatrickc N.: J. Dent. *31*, 261 (2003).
25. Peng Z., Gong J., Miao H.: J. Eur. Ceram. Soc. *24*, 2193 (2004).
26. Li H., Bradt R.C.: J. Mater. Sci. *28*, 917 (1993).
27. Csehová E., Andrejovská J., Limpichaipanit A., Dusza J., Tood R.: Kovove Mater. *49*, 119 (2011).
28. Park S S., Quinn J.B., Romberg E., Arola D.: Dent. Mater. *24*, 1477 (2008).
29. Low I.M., Duraman N., Mahmood U.: Mater. Sci. Eng. *28*, 243 (2008).
30. Bechtle S., Habelitz S., Klocke A., Fett T., Schneider G.A.: Biomaterials *31*, 375 (2010).
31. Bechtle S., Fett T., Rizzi G., Habelitz S., Klocke A., Schneider G.A.: Biomaterials *31*, 4238 (2010).
32. He L.H., Swain M.V.: J. Biomed. Mater. Res. A. *81*, 484 (2007).
33. Fox P.G.: J. Mater. Sci. *15*, 3113 (1980).
34. Smith B.L., Schaffer T.E., Viani M., Thompson J.B., Frederick N.A., Kindt J., Belchers A., Stucky G.D., Morse D.E., Hansma P.K.: Nature *399*, 761 (1999).
35. Fantner G.E., Hassenkam T., Kindt J.H., Weaver J.C., Birkedal H., Pechenik L., Cutroni J.A., Cidade G.A.G., Stucky G.D., Morse D.E., Hansma P.K.: Nat. Mater. *4*, 612 (2005).
36. Macho G.A. , Jiang Y., Spears I.R.: J. Hum. Evol. *45*, 81 (2003).
37. He L.H., Swain M.V.: J. Dent. *35*, 431 (2007).
38. Ashby M.F., Jones D.R.H.: *Engineering Materials: An Introduction to their Properties and Applications*, Pergamon Press, 1980.
39. Frost H.J., Ashby M.F.: *Deformation-Mechanism Maps: The Plasticity and Creep of Metals and Ceramics*, Pergamon Press, 1982.
40. Turner S.: *Creep of Polymeric Materials*, Elsevier Science Ltd., Oxford 2001.
41. Menčík, He L.H., Swain M.V.: J. Mech. Behav. Biomed. *2*, 318 (2009).
42. He L.H., Swain M.V.: J. Biomed. Mater. Res. A. *91*, 352 (2009).
43. Jafarzadeh T., Erfan M., Watt D.C.: J. Dent. *1*, 5 (2004).
44. El-Safty E., Silikas N., Akhtar R., Watt D.C.: Dent. Mater. *28*, 1171 (2012).